Effect of Terraces at the Interface on the Structural and Physical Properties of $La_{0.8}Sr_{0.2}MnO_3$ Thin Films *

Ya-Qing Feng(冯雅晴)[1], Kui-Juan Jin(金奎娟)[1,2**], Chen Ge(葛琛)[1], Xu He(何旭)[1], Lin Gu(谷林)[1], Zhen-Zhong Yang(杨振中)[1], Hai-Zhong Guo(郭海中)[1], Qian Wan(万骞)[1], Meng He(何萌)[1], Hui-Bin Lu(吕惠宾)[1], Guo-Zhen Yang(杨国桢)[1,2]

[1] *Institute of Physics, Chinese Academy of Sciences, Beijing 100190*
[2] *Collaborative Innovation Center of Quantum Matter, Beijing 100190*

(Received 21 March 2016)

Employing atomic force microscopy, transmission electron microscopy and the second harmonic generation technique, we carefully explore the structural properties of 6-unit-cell-thick $La_{0.8}Sr_{0.2}MnO_3$ films grown on $SrTiO_3$ with atomically flat TiO_2-terminated terraces on the surface. The results clearly demonstrate that the terraces on the surface of TiO_2-terminated $SrTiO_3$ can improve the layer-by-layer epitaxial growth of the manganite films, which results in uniform film coverage at the beginning of growth and thus reduces the substrate-induced disorder at or near the interface. Comparing the magnetic and transport properties of $La_{0.8}Sr_{0.2}MnO_3$ films with the thicknesses varying from 6 unit cells to 80 unit cells grown respectively on as-received $SrTiO_3$ and TiO_2-terminated $SrTiO_3$, it is found that these atomically flat terraces on the surface of TiO_2-terminated $SrTiO_3$ can greatly enhance the Curie temperature and conductivities of the ultrathin $La_{0.8}Sr_{0.2}MnO_3$ films with thickness less than 50 unit cells, while no obvious difference is detected in the magnetic and transport properties of the 80 unit-cell thick films.

PACS: 68.35.Ct, 75.75.−c, 73.63.−b, 68.37.Lp DOI: 10.1088/0256-307X/33/7/076801

The perovskite oxide $SrTiO_3$ (STO) is a widely used substrate material for epitaxial growth of functional thin films and nanostructures[1,2] due to the compatible lattice constants and thermal expansion coefficients between STO and those oxide materials.[3] Since STO has a stacked structure with two alternative kinds of SrO and TiO_2 perpendicular to the [001] direction,[3,4] the as-received STO (001) (A-STO) substrates generally present two types of termination, namely SrO or TiO_2. By chemical etching or other improved techniques,[5,6] TiO_2-terminated STO (T-STO) can be obtained with atomically flat and single terminated terraces on the surface of T-STO substrate. More interestingly, the surface of T-STO provides us with an intriguing playground for the appearance of a variety of novel phenomena.[7−11] A most famous example is the two-dimensional electron gas at the interface between $LaAlO_3$ (LAO) and T-STO observed by Ohtomo *et al.*[7] Therefore, this T-STO substrate has attracted continuing interest owing to the technological and scientific importance of the surface.

Meanwhile, the atomically flat terraces on the surface of T-STO also prove to be important for the epitaxial growth of high quality manganite films. Recent research[12] has shown that the metal-insulator transition (MIT) temperature of $La_{0.7}Ca_{0.3}MnO_3$ ultrathin film is increased by 20 K when using T-STO as opposed to the as-received ones, and that the thickness of the dead layer depends on the smoothness of the substrate. However, many related fundamental issues remain to be uncovered for manganite films grown on T-STO, such as the atomic structure of manganite films near the TiO_2-terminated terraces, and whether these atomically flat terraces on the surface of T-STO enhance the magnetic properties and conductivities of manganite films when the manganite films become thicker. In this work, we have carefully studied the structural properties of the 6-unit-cell-thick (u.c.) $La_{0.8}Sr_{0.2}MnO_3$ (LSMO) film grown on T-STO. Atomically flat terraces are observed from the surface topography of the film and the localization of the interface observed from the transmission electron microscope (TEM) image shows a unit-cell height of difference near the TiO_2-terminated terrace. In addition, the second harmonic (SH) measurement reveals that the surface symmetry of the 6-u.c.-thick film is consistent with that of the STO substrate. We have also compared the magnetic and transport properties of LSMO films with thicknesses varying from 6 u.c. to 80 u.c. grown on T-STO and A-STO, respectively. The result indicates that for the 6-u.c. and 30-u.c.-thick LSMO films grown on T-STO, both the Curie temperature T_c and conductivities are much higher than those grown on A-STO. However, this difference narrows down and almost disappears when gradually increasing the thickness of LSMO films from 6 u.c. to 80 u.c.

By chemical etching and thermal annealing in oxygen, the high-quality T-STO substrates with atom-

*Supported by the Strategic Priority Research Program (B) of Chinese Academy of Sciences under Grant No XDB07030200, the National High-Technology Research and Development Program of China under Grant No 2014AA032607, and the National Natural Science Foundation of China under Grant No 11404380.

**Corresponding author. Email: kjjin@iphy.ac.cn

© 2016 Chinese Physical Society and IOP Publishing Ltd

ically flat and single terminated terraces on the surface are obtained. More details of the treating method can be found in our early research.[3] $La_{0.8}Sr_{0.2}MO_3$ films were deposited on (001) cut A-STO and T-STO substrates by a laser molecular beam epitaxy (Laser-MBE) system (PASCAL) using a XeCl excimer laser (wavelength of 308 nm, pulse width of 20 ns, energy density of 2.18 J/cm^2, repetition of 2 Hz). The films were grown at 930℃ and the oxygen partial pressure was set to 30 Pa. The growth process was monitored in situ by reflective high-energy electron diffraction (RHEED) analysis allowing for precise control of the thickness at the unit cell scale and accurate characterization of the growth dynamics.

The surface morphology of the LSMO films were recorded by using a commercial atomic force microscopy (AFM) system (Asylum Research MFP3D). The atomic structure of the LSMO films was characterized by using an ARM-200CF (JEOL, Tokyo, Japan) transmission electron microscope (TEM) operated at 200 keV and equipped with double spherical aberration (Cs) correctors. The attainable resolution of the probe defined by the objective pre-field is 78 pm. In addition, we used the reflected second harmonic generation (SHG) to probe both the surface and the interface of the LSMO/STO heterostructures, and the experimental scheme and detailed descriptions have been reported in previous research.[13]

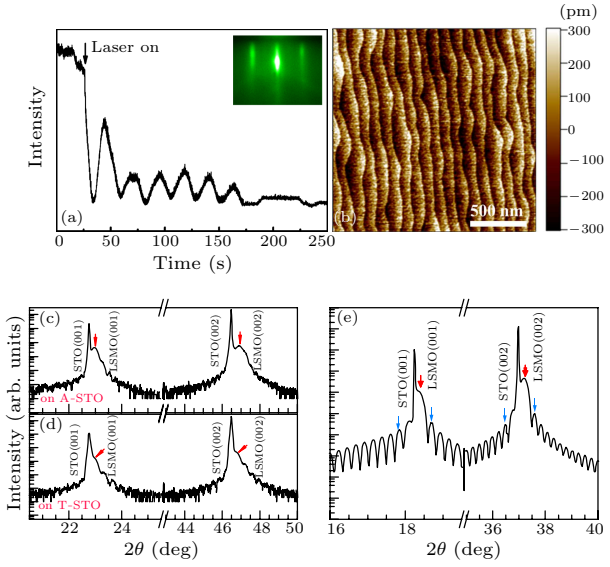

Fig. 1. (a) RHEED oscillations recorded during the growth of the 6 u.c. thick LSMO film grown on T-STO, and (b) AFM image of the 6 u.c. thick film grown on T-STO. (c, d) X-ray diffraction patterns of the 80 u.c. LSMO film grown on A-STO and on T-STO . The red arrows point at the diffraction peaks of the LSMO films. The wavelength of the x-ray is 1.54 Å. (e) Synchrotron-based x-ray diffraction patterns of the 80-u.c.-thick LSMO film grown on the T-STO. The red arrows point at the diffraction peaks of the LSMO films. The blue arrows indicate thickness fringes, showing a coherent interface between the LSMO film and the substrate, whose distance can be used to estimate the layer thickness.

The x-ray diffraction (XRD) patterns of all the LSMO films are obtained by the high resolution diffractometer (Rigaku, SmartLab, 9 kW) equipped with a Ge (220)×2 monochromator, and the XRD patterns of the 80-u.c.-thick LSMO films grown on A-STO and T-STO are given in Figs. 1(c) and 1(d). Only diffraction peaks from the substrate and the LSMO film are observed, confirming that the film is grown along the c-axis and has a single phase without impurities. We have also obtained the synchrotron-based XRD (SXRD) patterns of the LSMO films grown on T-STO by high-resolution Synchrotron x-ray diffractometry in the BL14B1 beam line of Shanghai Synchrotron Radiation Facility (SSRF), using a 1.24 Åx-ray with a Huber 5021 six-axis diffractometer. The SXRD pattern of the 80-u.c.-thick LSMO film grown on T-STO is shown in Fig. 1(e), and the satellite peaks located around the main LSMO peaks indicate a perfectly coherent interface between the film and the T-STO substrate.

The magnetization and resistivity measurements were performed by using a Quantum Design physical property measurement system (PPMS). The transport properties were measured in a four-probe configuration in the temperature range of 10–400 K. Platinum pads were deposited on the films and contacts were made by attaching platinum wires to the samples by using silver paste. Magnetic measurements were carried out with the magnetic field applied in plane. Temperature dependence of magnetization for all films was recorded with a small magnetic field of 200 Oe.

Figure 1(a) shows the RHEED oscillations of the 6-u.c.-thick film grown on T-STO recorded during the growth process, and the diffraction pattern of the film (inset of Fig. 1(a)) indicates a flat surface. The surface topography of the film is further characterized by the atomic force microscopy (AFM). As can be seen in the AFM image of the 6-u.c.-thick film (Fig. 1(b)), the surface consists of flat steps and terraces with an averaged width of about 112 nm. Therefore, we can obtain that the miscut angle of the substrate is about 0.06°. The rms roughness is about 300 pm.

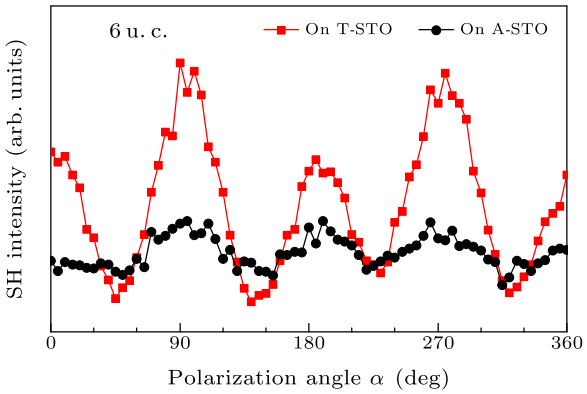

Fig. 2. The comparative SH intensity-dependent measurements on the polarization angle α for the 6-u.c.-thick LSMO films grown on T-STO and A-STO, respectively.

The surface symmetry of the 6-u.c.-thick LSMO

film grown on T-STO is investigated by using the optical reflected second harmonic generation (SHG) technique. The result is shown in Fig. 2, and the SH intensity of the 6-u.c.-thick film grown on A-STO has also been recorded for comparison. For the 6-u.c.-thick film grown on T-STO, the SH intensity dependence on the polarization angle α indicates that the LSMO film is with $4mm$ symmetry, which is consistent with the surface symmetry of the STO substrate.[13] This demonstrates uniform film coverage on the surface of T-STO. However, for the 6-u.c.-thick film grown on A-STO, the surface symmetry can be hardly determined since the SH intensity is rather weak. This means that the LSMO film grown on A-STO has a rough surface due to the non-uniform film coverage, and a less sharp interface compared with that of the film grown on T-STO. This comparative result illustrates that the terraces on the surface of the T-STO substrate can promote the layer-by-layer epitaxial growth in the initial growth process.

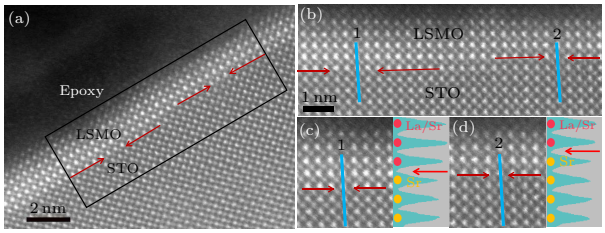

Fig. 3. (a) HAADF micrograph of the 6-u.c.-thick LSMO thin film near the step edge taken by an aberration-corrected STEM. (b) Zoomed image of the rectangular part in (a) with two blue bars marked with 1 and 2. The red arrows indicate where the STO/LSMO interface locates near the step edge. Here (c) and (d) show intensity line profiles of the blue bars marked with 1 and 2 in (b). The different contrasts of La and Sr provide exact chemical information and localization of the interface indicated by the red arrows in (c) and (d).

To investigate the atomic structure of the LSMO film grown on the step-and-terrace surface of the T-STO substrate, the high-angle annular-dark-field (HAADF) micrograph of the 6-u.c.-thick film is taken by using an aberration-corrected STEM (Fig. 3(a)). A row of tightly spaced atoms on the topmost LSMO layer can be seen in Fig. 3(a), with occasional atoms sticking out from the surface of the film. In the HAADF micrograph, the brightness is approximately proportional to Z^2, thus the darker area in Fig. 3(a) corresponds to the STO substrate, and the brighter one to the LSMO film. The abrupt contrast between STO and LSMO in Fig. 3(a) shows a well-defined interface marked by the red arrows in Fig. 3(a). A zoomed image of the rectangular part in Fig. 3(a) is presented in Fig. 3(b), and the intensity line profiles of the blue bars marked with 1 and 2 in Fig. 3(b) is correspondingly presented in Figs. 3(c) and 3(d). The different contrasts of La and Sr provide an accurate localization of the interface indicated by the red arrows in Figs. 3(a)–3(d). The localization of the LSMO/T-STO interface marked by the red arrows in Fig. 3 clearly shows a unit-cell height of difference near the edge of the TiO_2-terminated terrace.

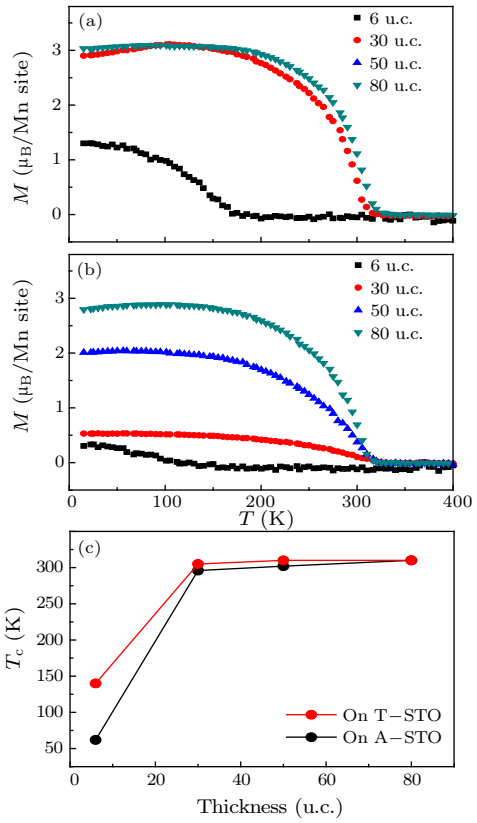

Fig. 4. The temperature dependence of magnetization (200 Oe, field cooling) of the LSMO films grown on T-STO (a) and on A-STO (b). (c) The comparative thickness dependence of the Curie temperature T_c for LSMO films grown on T-STO and A-STO, respectively.

The above results clearly demonstrate that the terraces on the surface of T-STO improve the layer-by-layer epitaxial growth of the ultrathin LSMO films, which leads to a uniform film coverage at the beginning of growth. Next, to explore the effect of terraces at the LSMO/STO interface on the magnetic properties of LSMO films with various thicknesses, we have compared the magnetic properties of LSMO films grown on T-STO and A-STO with the same thickness. Figures 4(a) and 4(b) show the temperature dependence of magnetization (200 Oe, field cooling) of LSMO films grown on T-STO and A-STO, respectively. It can be seen from Fig. 4(a) that the magnetization becomes weaker with decreasing the temperature below 105 K for films grown on T-STO with thickness larger than 6 u.c. film. This phenomenon indicates that the spin of the Mn ions is slightly canted or some antiferromagnetically coupled regions appeared in the films below 105 K, which can be attributed to the cubic-to-tetragonal phase transition at $T_{CT} = 105$ K in the substrate STO.[14,15] Indeed, recent investigations have reported that the magnetization of $La_{1-x}Sr_xMnO_3$ thin films grown on STO (100) shows distinct changes upon crossing T_{CT}

which was triggered by the structural transition occurring in STO.[15–18] Moreover, since the doping level of LSMO films deviates from the optimal doping level of $x = 0.33$, the magnetic structure of the LSMO layer is more sensitive to the tiny structural changes of the STO substrate.[14] Detailed explanation for this anomaly in $M(T)$ at 105 K can be found in our early research.[17]

However, no anomaly in $M(T)$ at 105 K can be observed in LSMO films grown on A-STO (Fig. 4(b)). This is caused by the existence of defects and disorder at or near the LSMO/A-STO interface which further distributes throughout the films and thus dominates the low temperature magnetization of films grown on A-STO. Therefore, the effect of STO phase transition at 105 K does not play a significant role in the low-temperature magnetic properties of LSMO films grown on A-STO.

The thickness-dependent Curie temperature T_c of LSMO films deposited on T-STO and A-STO is shown in Fig. 4(c). Here we define T_c as the temperature at which (dM/dT) reaches the maximum.[19] As can be seen in Fig. 4(c), for films grown on either T-STO or A-STO, a significant increase in T_c can be detected when the thickness of the film is increased from 6 u.c. to 30 u.c. For LSMO films grown on T-STO, T_c of the 30 u.c. thick film is increased to 305 K, which is comparable to that of the bulk $La_0.8Sr_0.2MnO_3$,[20], and no obvious changes can be observed in T_c when the thickness of the film is further increased to 50 or 80 u.c. Meanwhile T_c of the films grown on A-STO shows a slight increase from 290 to 307 K when the thickness of the film is increased from 30 u.c. to 80 u.c. Moreover, we can see from Fig. 3(c) that T_c of the 6 u.c. thick film grown on T-STO is about 78 K higher than that of the 6-u.c.-thick film grown on A-STO, which indicates that the TiO_2-terminated terraces on the surface of T-STO can greatly enhance the magnetic properties of the ultrathin films. However, the difference in T_c between films of the same thickness grown on T-STO and A-STO narrows down and disappears when the thickness is gradually increased to 80 u.c.

The comparative temperature-dependent resistivities for LSMO films grown on T-STO and A-STO with various thicknesses are given in Fig. 5. An insulator-metal phase transition is found at 180 K in the 6-u.c.-thick LSMO film grown on T-STO, while the 6-u.c.-thick film grown on A-STO is insulating in the whole temperature range with larger resistivities compared with that of the film grown on T-STO. This result indicates that the terraces at the interface can decrease the thickness of the dead layer and improve the conductivities of LSMO films. When the thickness is increased to 30 u.c., both films grown on T-STO and A-STO display an insulator-metal phase transition and the difference in resistivities becomes smaller. When the film thickness is further increased to 50 u.c. and 80 u.c., the difference in resistivities between films grown on A-STO and that on T-STO gradually disappears.

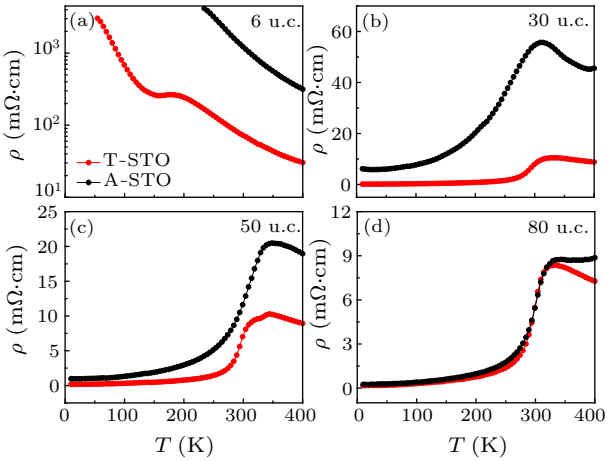

Fig. 5. (a)–(d) The comparative temperature dependence of resistivities of the 6 u.c., 30 u.c., 50 u.c. and 80-u.c.-thick LSMO films grown on T-STO and A-STO, respectively.

The magnetic and electronic measurements both demonstrate that the TiO_2-terminated terraces on the surface of T-STO substrate can significantly improve the magnetic and transport properties of the ultrathin LSMO films, which can be attributed to the following two aspects. First of all, compared with as-received STO, the TiO_2-terminated STO features a surface with atomically flat terraces which promote the layer-by-layer epitaxial growth in the initial growth process. This is evidenced by the atomically flat terraces observed from the surface topography of the 6-u.c.-thick LSMO film (Fig. 1(a)). This layer-by-layer epitaxial growth results in a uniform film coverage,[21] thus fewer defects will be induced at or near the interface. Another important reason is that, compared with A-STO possessing two types of terminations, T-STO has a single TiO_2-terminated surface. When the LSMO film is deposited on the surface of T-STO, the MnO_2 planes grow uniformly on the surface of the La(Sr)O plane and thus reduces the distortion of oxygen octahedral.[4,22] As a result, it enhances the double exchange interaction in ultrathin LSMO films grown on T-STO, which improves the magnetic and transport properties.

However, when the LSMO film becomes thicker, the properties of the film grown on T-STO or A-STO are less affected by the interface defects and are enhanced with increasing thickness and become bulk-like. Then the properties of the LSMO film remains the same when the thickness is further increased. Therefore, no obvious difference can be seen in the magnetization and conductivities of the 80-u.c.-thick LSMO film grown on T-STO and A-STO since both films display bulk-like properties.

In addition, by studying the surface morphology of the LSMO films we have found that the film grown on T-STO gradually deviates from the ideal layer-

by-layer epitaxial growth with increasing the thickness and thus leads to non-uniform film coverage. As shown in Fig. 6, terraces can be hardly observed from the surface morphology of the 50-u.c.-thick film grown on T-STO, and some rather large islands appeared on the surface of the 80-u.c.-thick film. As a result, disorders such as defects or inhomogeneities are induced in the films.[23] However, as can be seen in Fig. 4(c), T_c of 50 and 80-u.c.-thick LSMO films has nearly the same value as that of the 30-u.c.-thick film, which indicates that the properties of the LSMO films with relatively large thickness are not distinctly affected by the type of disorder which is induced by non-uniform film coverage.

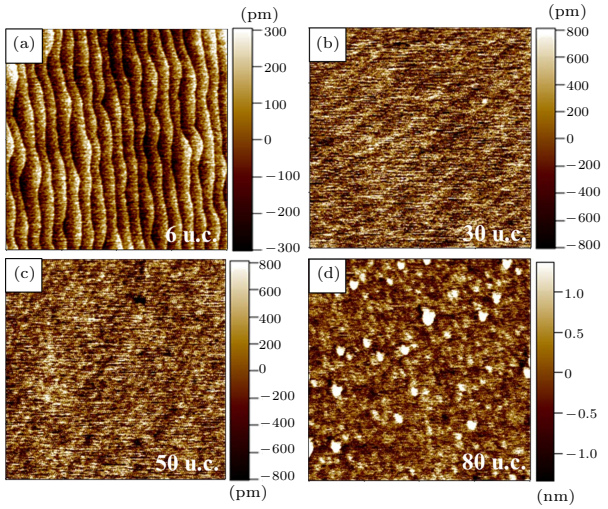

Fig. 6. (a)–(d) AFM images of LSMO films grown on T-STO with thicknesses of 6 u.c. (a), 30 u.c. (b), 50 u.c. (c) and 80 u.c. (d).

In conclusion, our results clearly demonstrate that the atomically flat terraces on the surface of TiO_2-terminated STO can greatly improve both the magnetic and transport properties of ultrathin LSMO films, due to the perfect layer-by-layer epitaxial growth in the initial growth process and less substrate-induced disorder at the LSMO/T-STO interface. However, when the LSMO films become thicker, the properties of the films are less affected by the interface defects and gradually become bulk-like. Therefore, the difference between properties of the films grown on T-STO and A-STO gradually narrows down and disappears with increasing the thickness. The present work is helpful to understand the crucial role of atomically flat terraces on the surface of $SrTiO_3$ in the growth of high quality manganite films, and similar results can be applied to the growth of manganite films on other substrates with perovskite structure.

References

[1] Jiang Q D and Zegenhagen J 1995 *Surf. Sci.* **338** L882
[2] Silly F and Castell M R 2005 *Appl. Phys. Lett.* **87** 213107
[3] Wang X, Fei Y Y, Lu H B, Jin K J, Zhu X D, Chen Z H, Zhou Y L and Yang G Z 2005 *Sci. Chin. Ser.* G **48** 459
[4] Bibes M, Valencia S, Balcells L, Martínez B, Fontcuberta J, Wojcik M, Nadolski S and Jedryka E 2002 *Phys. Rev.* B **66** 134416
[5] Seo S S A, Choi W S, Lee H N, Yu L, Kim K W, Bernhard C and Noh T W 2007 *Phys. Rev. Lett.* **99** 266801
[6] Kim J S, Seo S S A, Chisholm M F, Kremer R K, Habermeier H U, Keimer B and Lee H N 2010 *Phys. Rev.* B **82** 201407
[7] Ohtomo A and Hwang H Y 2004 *Nature* **427** 423
[8] Dikin D A, Mehta M, Bark C W, Folkman C M, Eom C B and Chandrasekhar V 2011 *Phys. Rev. Lett.* **107** 056802
[9] Ohtomo A, Muller D A, Grazul J L and Hwang H Y 2002 *Nature* **419** 378
[10] Biscaras J, Bergeal N, Kushwaha A, Wolf T, Rastogi A, Budhani R C and Lesueur J 2010 *Nat. Commun.* **1** 89
[11] Wang M, Ou Y B, Li F S, Zhang W H, Tang C J, Wang L L, Xue Q K and Ma X C 2014 *Acta Phys. Sin.* **63** 027401
[12] Padhan P, Pandey N K, Srivastava S, Rakshit R K, Kulkarni V N and Budhani R C 2000 *Solid State Commun.* **117** 27
[13] Zhao R Q, Jin K J, Guo H Z, Lu H B and Yang G Z 2013 *Sci. Chin. Phys. Mech. Astron.* **56** 2370
[14] Fontcuberta J, Skumryev V, Laukhin V, Granados X and Salje E K H 2015 *Sci. Rep.* **5** 13784
[15] Salje E K H, Aktas O, Carpenter M A, Laguta V V and Scott J F 2013 *Phys. Rev. Lett.* **111** 247603
[16] Rondinelli J M, May S J and Freeland J M 2012 *MRS Bull.* **37** 261
[17] Feng Y Q, Jin K J, Gu L, He X, Ge C, Zhang Q H, He M, Guo Q L, Wan Q, He M, Lu H B and Yang G Z 2016 *Sci. Rep.* **6** 22382
[18] Pesquera D, Skumryev V, Sanchez F, Herranz G and Fontcuberta J 2011 *Phys. Rev.* B **84** 184412
[19] Wang C, Jin K J, Gu L, Lu H B, Li S M, Zhou W J, Zhao R Q, Guo H Z, He M and Yang G Z 2013 *Appl. Phys. Lett.* **102** 252401
[20] Urushibara A, Moritomo Y, Arima T, Asamitsu A, Kido G and Tokura Y 1995 *Phys. Rev.* B **51** 14103
[21] Luo Z Y, Tang J, Ma B, Zhang Z Z, Jin Q Y and Wang J P 2012 *Chin. Phys. Lett.* **29** 127501
[22] Ge C, Jin K J, Gu L, Peng L C, Hu Y S, Guo H Z, Shi H F, Li J K, Wang J O, Guo X X, Wang C and He M 2015 *Adv. Mater. Interfaces* **2** 1500407
[23] Moreo A, Mayr M, Feiguin A, Yunoki S and Dagotto E 2000 *Phys. Rev. Lett.* **84** 5568